AMERICAN SOCIETY FOR MICROBIOLOGY | Journal of Bacteriology

Bacteriology | Full-Length Text

Characterization of Ssc, an *N*-acetylgalactosamine-containing *Staphylococcus aureus* surface polysaccharide

Mei G. Lei,[1] Matthew A. Jorgenson,[1] Emily J. Robbs,[1] Ian M. Black,[2] Stephanie Archer-Hartmann,[2] Sergei Shalygin,[2] Parastoo Azadi,[2] Chia Y. Lee[1]

AUTHOR AFFILIATIONS See affiliation list on p. 13.

ABSTRACT Whole genome sequencing has revealed that the genome of *Staphylococcus aureus* possesses an uncharacterized 5-gene operon (SAOUHSC_00088–00092 in strain 8325 genome) that encodes factors with functions related to polysaccharide biosynthesis and export, indicating the existence of a new extracellular polysaccharide species. We designate this locus as *ssc* for staphylococcal surface carbohydrate. We found that the *ssc* genes were weakly expressed and highly repressed by the global regulator MgrA. To characterize Ssc, Ssc was heterologously expressed in *Escherichia coli* and extracted by heat treatment. Ssc was also conjugated to AcrA from *Campylobacter jejuni* in *E. coli* using protein glycan coupling technology (PGCT). Analysis of the heat-extracted Ssc and the purified Ssc-AcrA glycoconjugate by tandem mass spectrometry revealed that Ssc is likely a polymer consisting of *N*-acetylgalactosamine. We further demonstrated that the expression of the *ssc* genes in *S. aureus* affected phage adsorption and susceptibility, suggesting that Ssc is surface-exposed.

IMPORTANCE Surface polysaccharides play crucial roles in the biology and virulence of bacterial pathogens. *Staphylococcus aureus* produces four major types of polysaccharides that have been well-characterized. In this study, we identified a new surface polysaccharide containing N-acetylgalactosamine (GalNAc). This marks the first report of GalNAc-containing polysaccharide in *S. aureus*. Our discovery lays the groundwork for further investigations into the chemical structure, surface location, and role in pathogenesis of this new polysaccharide.

KEYWORDS *Staphylococcus aureus*, polysaccharides, N-acetylgalactosamine, Ssc

Despite advancements in healthcare delivery, *Staphylococcus aureus* remains a significant human pathogen in hospital and community settings. The organism is capable of producing a wide array of virulence factors that contribute to its pathogenicity. Treatments for serious *S. aureus* infections are largely limited to antibiotic therapy. However, *S. aureus* can readily acquire antibiotic resistance genetically as well as become tolerant to antibiotics upon biofilm formation (1).

Surface polysaccharides play an important role in bacterial physiology, virulence, and pathogenesis. In *S. aureus*, cell wall peptidoglycan, teichoic acids, capsular polysaccharide, and polysaccharide intracellular adhesion (PIA) have been extensively characterized. Teichoic acids and PIA are involved in biofilm formation, whereas capsules are involved in immune evasion by obstructing host phagocytic cells from assessing bacterial surfaces (2). PIA has also been reportedly involved in immune evasion (3).

Genome sequencing has revealed an uncharacterized 5-gene operon in the genome of *S. aureus*, with genes predicted to encode proteins involved in polysaccharide biosynthesis and export (4). This suggests the existence of a new extracellular polysaccharide species. The five genes, SAOUHSC_00088–00092 (strain 8325), are annotated

Editor Tina M. Henkin, Ohio State University, Columbus, Ohio, USA

Address correspondence to Chia Y. Lee, clee2@uams.edu.

The authors declare no conflict of interest.

See the funding table on p. 13.

Received 11 February 2024
Accepted 8 April 2024
Published 7 May 2024

Copyright © 2024 American Society for Microbiology. All Rights Reserved.

Downloaded from https://journals.asm.org/journal/jb on 25 June 2025 by 45.3.79.59.

based on homology to known enzymes as UDP-glucose (galactose) 4-epimerase, UDP-phosphate *N*-acetylgalactosaminyl-1-phosphate transferase, glycosyl transferase, polysaccharide polymerase, and membrane exporter, respectively. In this study, we provide evidence that this 5-gene locus is responsible for the production of a surface-exposed polysaccharide, which we named Ssc for staphylococcal surface carbohydrate. The five genes were designated *sscA* through *sscE*. Our results suggest that Ssc is a polysaccharide located on the *S. aureus* surface. Analysis of the purified polysaccharide expressed in *Escherichia coli* suggests that Ssc is likely a polymer consisting of *N*-acetylgalactosamine (GalNAc).

RESULTS

Expression of the *ssc* genes

The *ssc* locus consists of 5 genes that are closely arranged, suggesting an operonic structure. The locus is not part of a known genetic element (Fig. S1). An NCBI BLAST (National Center for Biotechnology Information Basic Local Alignment Search Tool) search showed that these genes are highly conserved among *S. aureus* strains. KEGG (Kyoto Encyclopedia of Genes and Genomes) ortholog analysis showed that all five annotated protein sequences are highly homologous in all 53 sequenced strains (at least 94% identity). As the *ssc* genes were annotated as putative polysaccharide genes, to determine whether the *ssc* locus encodes for a polysaccharide, we purified the crude carbohydrate from 8325-4, a phage-free strain derived from 8325, and the isogenic *ssc* deletion mutant by heat treatment of the bacterial cells grown overnight. The heat-extracted fractions were then further digested with DNase I and RNase A to remove DNA and RNA, respectively, and proteinase K to remove proteins. The crude extracts, consisting mostly of carbohydrates, were subject to SDS-PAGE analysis followed by silver staining. Polysaccharide-like ladder bands were observed in both the wild-type and the *ssc* mutants (CYLA946), with similar quantities between the two (Fig. 1A, lanes 1 and 2). This suggests that *ssc* genes are expressed at a very low level, indicating that the *ssc* locus does not have a significant impact on total carbohydrate production. It should be noted here that using exponential or early stationary phase cultures did not show differences between the wild-type and the *ssc* mutants.

The *ssc* locus consists of five genes that are closely arranged, suggesting an operonic structure. To study the expression of the *ssc* genes in S. *aureus*, we characterized the promoter activity of the operon. The putative promoter region upstream of the first gene, *sscA*, was fused to the superfolder green fluorescence protein gene (*sfgfp*) resulting in plasmid pMLE283. As shown in Fig. 1B, we found that the *ssc* promoter (P*ssc*) activity in 8325-4 was only slightly above the background control, indicating that the *ssc* genes are expressed at a very low level in this strain. In a previous gene profiling study (5), we found that all the *ssc* genes were downregulated by a global regulator, MgrA. To confirm whether the *ssc* genes are repressed by MgrA, we transformed pMLE283 to 8325-4 *mgrA* mutant (CYL13008). As shown in Fig. 1B, P*ssc* activity increased drastically in the *mgrA* mutant, indicating that the *ssc* operon is highly repressed by MgrA. It has been reported that MgrA binds to a consensus sequence of (A/T)GTTGT (6, 7); however, we found that no sequence matched exactly to the consensus in the putative *ssc* promoter region.

Given that MgrA is a strong repressor of *ssc* genes, we further compared the crude carbohydrate extracts between the *mgrA* mutant and the *mgrA-ssc* double mutant. The results (Fig. 1A, lanes 3 and 4) revealed distinct bands in the *mgrA* mutant but not in the *mgrA-ssc* double mutant (indicated by arrows). Although these bands were faint, they likely represent the putative carbohydrate expressed from the *ssc* locus. Since strain 8325-4 can produce PIA and teichoic acids but does not produce capsular polysaccharides (8–11), we presume that the background bands are composed of PIA and teichoic acids or other not yet identified carbohydrates.

Downloaded from https://journals.asm.org/journal/jb on 25 June 2025 by 45.3.79.59.

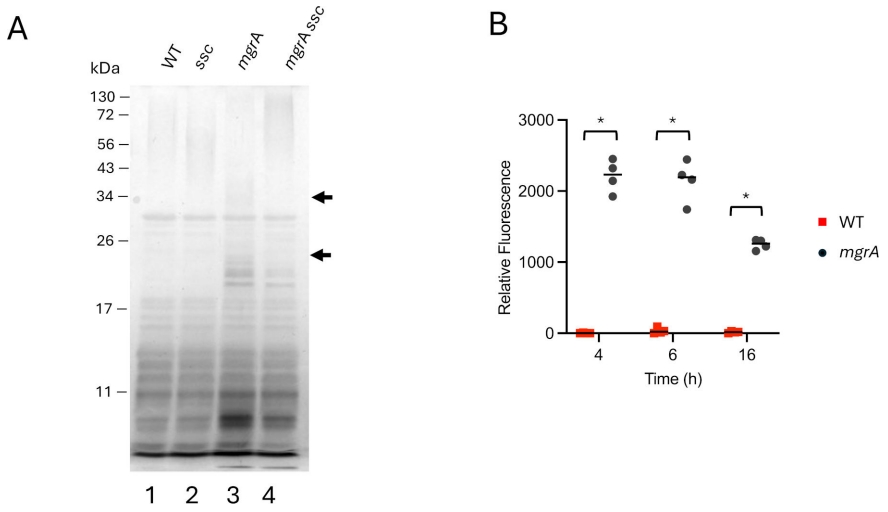

FIG 1 Expression of Ssc in *S. aureus*. (A) Heat-extracted *S. aureus* surface carbohydrates were analyzed by SDS-PAGE (15%) followed by silver staining. WT, 8325-4; *ssc*, CYLA946; *mgrA*, CYL12670; *mgrA ssc*, CYLA958. Putative Ssc bands are indicated by arrows. (B) Effect of MgrA on P*ssc* promoter activities by sfGFP reporter assay. Red squares, WT, 8325-4(pMLE283); black dots, *mgrA* mutant, CYL13008(pMLE283). Statistical significance relative to the wild type was analyzed by Student *t*-test ($n = 4$). *, $P < 0.0001$.

Ssc polymer contains *N*-acetylgalactosamine

To identify the putative polysaccharide encoded by the *ssc* locus, the entire *S. aureus ssc* operon was cloned into pBBR1MCS-2, resulting in pMLE254, and expressed in *E. coli* MG1655. Polysaccharides from the Ssc expressing strain (CYLE260) and the vector control strain (CYLE259) were prepared as described in Materials and Methods. Trichloroacetic acid (TCA) soluble and ethanol-precipitated polysaccharide fractions were analyzed by 13% SDS-PAGE and silver staining. As shown in Fig. 2A, we found distinct ladder-like bands from CYLE260 that were not present in the control, suggesting that these bands are composed of polysaccharides. To determine the presumptive polysaccharides, the TCA and ethanol-treated polysaccharide extracts from CYLE260 and CYLE259 strains were sent to the Complex Carbohydrate Research Center (CCRC) at the University of Georgia for carbohydrate composition analysis. Table 1 and Fig. S2 (in the supplemental

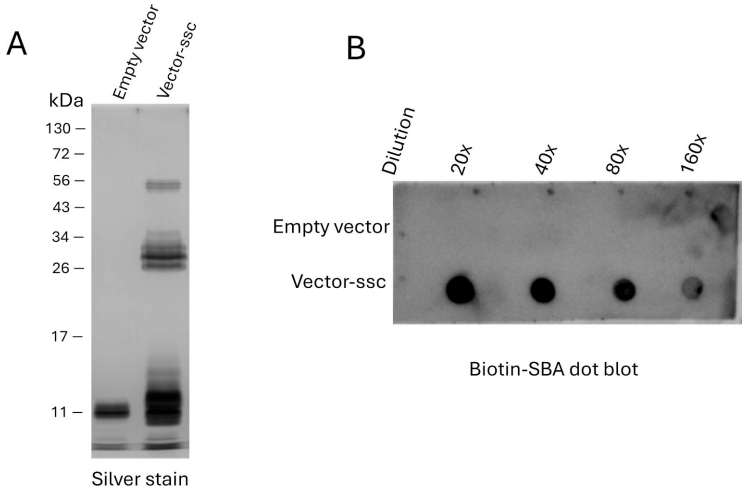

FIG 2 Expression of Ssc in *E. coli*. Carbohydrates from strains CYLE259 carrying pBBR1MCS-2 vector and CYLE260 carrying pBBR1MCS-2-*ssc* were analyzed by SDS-PAGE, followed by silver-staining (A) or blotting with biotin-SBA (B).

Downloaded from https://journals.asm.org/journal/jb on 25 June 2025 by 45.3.79.59.

TABLE 1 Relative mole percent and carbohydrate content of microbial samples

Glycosyl residue	E259 control	E260 Ssc
Ribose (Rib)	79.7	53.3
Mannose (Man)	3.2	2.9
Galactose (Gal)	0.6	2.1
Glucose (Glc)	14.0	22.3
N-acetylgalactosamine (GalNAc)	n.d.[a]	6.0
Heptose (Hep)	1.6	8.9
2-keto-3-deoxy-D-mannooctanoic acids (Kdo)	0.7	4.6
Mannitol	0.3	n.d.
%CHO[b]	10.1	8.0

[a]Not detected.
[b]Carbohydrate percentage.

materials) show the relative mole percentage and carbohydrate content of CYLE259 and CYLE260. Both strains yielded polysaccharide fractions containing galactose, heptose, and 2-keto-3-deoxy-D-mannooctanoic acid (kdo), whereas GalNAc was found in CYLE260 carrying the *ssc* genes but not in the vector control strain CYLE259. These results suggest that the *ssc* operon is responsible for the synthesis of GalNAc. The identification of GalNAc is consistent with the predicted *ssc* gene functions. The observation of the ladder-like banding patterns further suggests that Ssc is likely a polymer consisting of GalNAc. Since soybean agglutinin (SBA) binds specifically to GalNAc and galactose but much more strongly to the former (12), to confirm the presence of GalNAc, we used a biotinylated SBA (biotin-SBA) binding assay. As shown in Fig. 2B, we found binding of biotin-SBA to the polysaccharide extract of CYLE260 but not to CYLE259, confirming that *ssc* locus is required for the synthesis of a GalNAc-containing glycan.

To further characterize the Ssc polysaccharide, we generated a Ssc glycoprotein conjugate using protein glycan coupling technology (PGCT) (13). PGCT is a recombinant process that involves the biological conjugation of heterologous polysaccharides to carrier proteins in engineered strains of *E. coli*. PGCT involves three components (glycan, carrier protein, and coupling enzyme), which are usually encoded on plasmids. To this end, we transformed pBBR1MCS-2-ssc (pMLE254) into the *E. coli* strain MAJ1625 resulting in strain MAJ1626, i.e., MG1655 Δ*wecA* Δ*waaL* λDE3 (pMAJ205). This strain is lysogenized with λDE3 to induce expression from pMAJ205 (a derivative of pACYCDuet-1). Plasmid pMAJ205 expresses *E. coli* codon-optimized versions of the PglB oligosaccharyltransferase and the AcrA carrier protein from *Campylobacter jejuni*. AcrA was modified at the N-terminus with the signal peptide from DsbA (for periplasmic expression) and four tandem repeats of the DQNAT glycosylation motif (for N-glycosylation) (14). AcrA was also modified at the C-terminus with four glycosylation motifs, as well as a hexahistidine tag for purification. In this system, PglB transfers Ssc structures to N-glycosylation sites in our AcrA variant (AcrA-His_6) in the periplasm. The chassis for our PGCT system is a derivative of *E. coli* MG1655 deleted for the O-antigen WaaL ligase (to prevent Ssc from being transferred by PglB onto lipid-A-core) and the initiating glycosyltransferase WecA (to prevent PglB from transferring enterobacterial common antigen).

To demonstrate that the Ssc polysaccharide contains GalNAc, Ssc-AcrA-His_6 glycoconjugates were prepared from the Ssc-expressing *E. coli* strain (CYLE277) as described in Materials and Methods (strain CYLE276 was the negative control). Cell pellets were either lysed with SDS sample buffer or lysed and subjected to His-tag protein purification. The samples were resolved with 11% SDS-PAGE, transferred to PVDF membrane, and blotted either with biotin-SBA (Fig. 3A) or with anti-His mouse mAb (Fig. 3B). The results showed that biotin-SBA bound to the bands in strain CYLE277 expressing Ssc (lanes 2 and 4 in Fig. 3A) but not in strain CYLE276 containing the vector only (Fig. 3A, lanes 1 and 3), indicating that the *ssc* genes are responsible for producing components that can be recognized by SBA. In the western blot using anti-His mAb, we found a prominent band above the 43 kDa marker that was specific to strain CYLE277, which is

Downloaded from https://journals.asm.org/journal/jb on 25 June 2025 by 45.3.79.59.

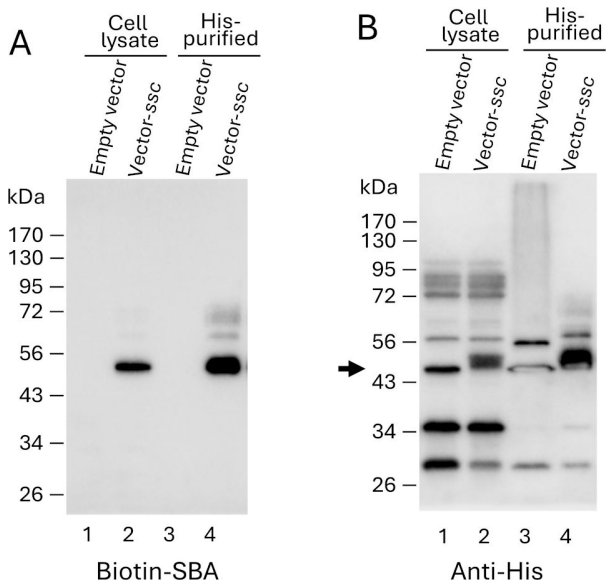

FIG 3 Glycosylation of AcrA-His$_6$ with ssc. Whole cell lysates and His-affinity-purified fractions were prepared from CYLE276 containing pBBR1MCS-2 vector and CYLE277 containing pBBR1MCS-2-*ssc*. Two microliters of the whole cell lysates (lanes 1 and 2) and 0.2 µL of His-affinity-purified fractions (lanes 3 and 4) were resolved with 11% SDS-PAGE, transferred to polyvinylidene fluoride (PVDF) paper, and blotted with biotin SBA (A) or blotted with mouse anti-His mAB to detect glycan-ArcA-His$_6$ (B). Arrow indicates ArcA-His$_6$ (49.4 kDa).

larger than the AcrA-His$_6$ protein indicated by an arrow (compare lanes 1 and 2 in Fig. 3B), suggesting that the GalNAc is conjugated to AcrA-His$_6$. For the His-bind-purified fractions blotted with anti-His mAb, additional faint bands specific to CYLE277 between 56 kDa and 72 kDa markers were found (Fig. 3B, lanes 3 and 4). These bands were also found in the blot against SBA (lane 4, Fig. 3A), suggesting that there are additional larger AcrA-His$_6$ conjugated glycans.

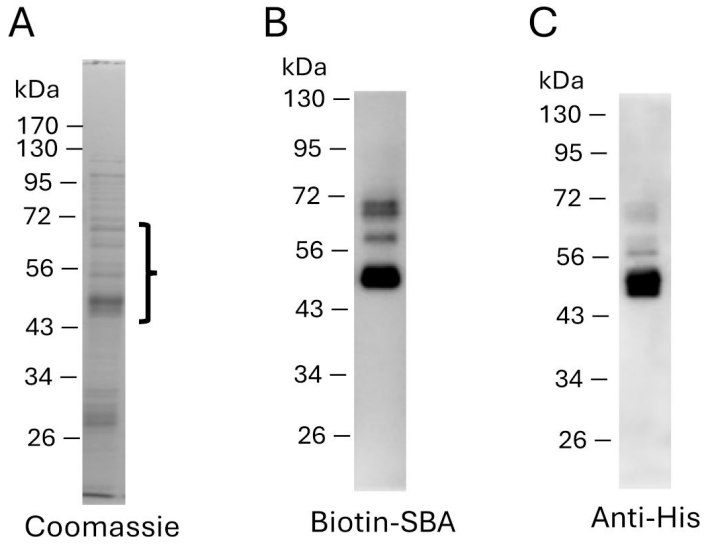

FIG 4 Purification of Ssc-AcrA-His$_6$ glycan. His-bind resin (Novagen) was used to isolate AcrA-His$_6$ and Ssc-AcrA-His$_6$ conjugates. Samples were resolved with 10% SDS-PAGE and stained with Coomassie Blue G250 (A), transferred to PVDF paper, and blotted with biotin-SBA (B) or with mouse anti-His mAB (C). Bracket indicates the gel portion excised for glycoproteomics and polysaccharide linkage analysis.

Downloaded from https://journals.asm.org/journal/jb on 25 June 2025 by 45.3.79.59.

To determine glycosylation by glycoproteomics, we purified the Ssc-AcrA-His_6 glycoconjugates from a 24 h culture of CYLE277 using His-bind resin. A small quantity of the samples (2 µL) was resolved in 10% SDS-PAGE and stained with Coomassie Blue (Fig. 4A), which revealed multiple bands. To approximate the positions of the Ssc-AcrA-His_6 conjugates, we further carried out western blotting with 0.2 µL sample using biotin-SBA and anti-His antibodies (Fig. 4B and C). A total of 80 µL of the sample was resolved in preparative SDS-PAGE gel (four lanes) and the portions corresponding to the 45–70 kDa range were excised and sent to the CCRC for in-gel glycoproteomic analysis. The results (see Fig. S3 in the supplemental materials) showed that all glycosylation sites were occupied with glycans. Examples of the tandem mass spectrometry (MS/MS) spectrum are shown in Fig. S4 and S5. Multiple *N*-acetyl-hexosamines (HexNAcs) were detected, most of which are low molecular weight (less than four carbohydrate units). Singly and doubly methylated polysaccharides were observed. These results suggest that the Ssc glycans in the glycoconjugates are mostly short polymers composed of HexNAcs, consistent with the carbohydrate composition analysis described above.

In an attempt to determine the linkage of GalNAc in the Ssc, N-glycans were released from the Ssc-AcrA-His_6 glycoconjugates by enzymatic digestion and subjected to glycomic analysis at the CCRC. However, we were unable to conclusively determine the linkage of the polysaccharides, despite using sample quantity 22-fold larger than that used in the glycoproteomic analysis mentioned above. Efforts to determine the Ssc structure are currently underway.

Ssc is surface-exposed

Surface polysaccharides play an important role in the interaction between bacterial surfaces and the environments, including the interaction of bacteria with phages (15). To determine whether Ssc is surface-exposed in *S. aureus*, we assessed the impact of Ssc on phage adsorption and the subsequent induction of cell lysis of *S. aureus*. Despite attempts to construct a *ssc*-complemented strain, the whole *ssc* locus could

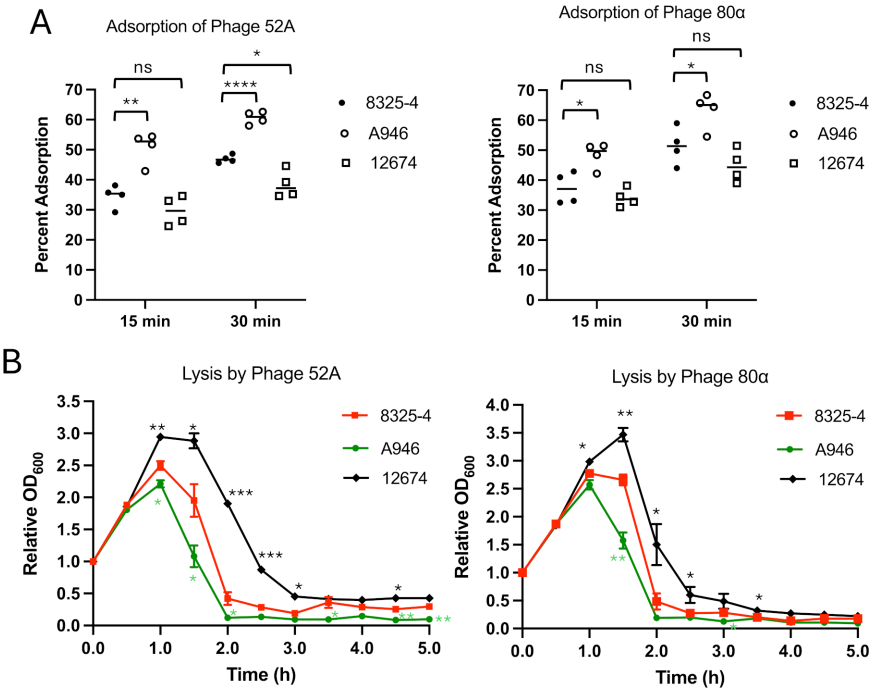

FIG 5 Surface-exposed Ssc. (A) Phage adsorption to *S. aureus* 8325-4 and its isogenic derivatives (n = 4). (B) Bacterial growth in the presence of phage (n = 3). CYLA946, *ssc* deletion mutant; CYL12674, Ssc overexpression strain. Statistical significance relative to the wild type was analyzed by Student t-test. *, $P < 0.05$; **, $P < 0.01$; ***, $P < 0.001$; ****, $P < 0.0001$; ns, not significant.

Downloaded from https://journals.asm.org/journal/jb on 25 June 2025 by 45.3.79.59.

not be cloned into the *ssc* mutant CYLA946. As an alternative, we constructed a strain (CYL12674) in which a constitutive promoter P*cap*1 (16) was inserted immediately upstream of the *sscA* gene (SAOUHSC_00088) in the 8325-4 chromosome. As shown in Fig. 5A, the adsorption of both phages 52A and 80α increased in the absence of Ssc, whereas the expression of Ssc under P*cap1* in CYL12674 led to a slight reduction of absorption compared with the wild-type strain 8325-4 (only the adsorption of 52A at 30 min is statistically significant). In contrast, the *ssc* mutant strain CYLA946 and the P*cap1-ssc* strain CYL12674 have the lowest and highest rate of lysis, respectively, by both phages (Fig. 5B). All staphylococcal phages attach to the wall teichoic acid or lipoteichoic acid (17, 18), which can be blocked by surface polysaccharides. Therefore, the results showing that Ssc reduced phage adsorption and the subsequent cell lysis suggest that Ssc is expressed and exposed on the surfaces of *S. aureus*.

To further show that the Ssc is surface-exposed, we labeled the whole *S. aureus* cells with fluorescein isothiocyanate-labeled SBA (FITC-SBA) and examined the image in a fluorescence microscope or using dot blot analysis. As shown in Fig. 6A, fluorescence was detected only on the *mgrA* mutant, particularly at sites of division. Interestingly, only about 10% of the cells were labeled. Phenotypic heterogeneity seems to be common for surface polysaccharides as similar cell variation of capsular polysaccharides has been reported previously (reviewed in reference 19). In the dot blot analysis, we found almost no labeling of FITC-SBA to either the wild-type or the *ssc* mutant, whereas the *mgrA* mutant showed strong binding (Fig. 6B). However, a detectable signal was found in the *mgrA ssc* mutant, suggesting that loss of MgrA may promote the expression of a component(s) capable of binding to SBA. Overall, the results in Fig. 6A and B demonstrate that Ssc is located on the cell surface of *S. aureus*.

To demonstrate that Ssc is attached to the *S. aureus* cell wall, we prepared the cell-wall fractions from 8325-4 and its isogenic mutants, including Δ*ssc*, Δ*mgrA*, and Δ*ssc*Δ*mgrA*. The cell wall fractions were further treated with proteinase K to remove contaminated proteins, spotted to nitrocellulose paper, and probed with biotin-SBA. The results in Fig. 6C showed that GalNAc was strongly detected in the *mgrA* mutant but barely detectable in the wild type, as expected. These results indicate that GalNAc is associated with the cell wall and that *ssc* genes are responsible for the synthesis of GalNAc in *S. aureus*.

DISCUSSION

S. aureus produces four major types of polysaccharides on bacterial surfaces that have been previously characterized. Here, we describe a new surface polysaccharide that is likely a polymer of GalNAc. Although at this stage we could not rule out the presence of other sugar components in Ssc, evidence for this conclusion is multi-fold. First, the five genes, which we designated as *sscA-E*, are annotated to be involved in polysaccharide biosynthesis and export. Second, expression of the five *ssc* genes in *E. coli* surrogate resulted in SDS-PAGE pattern typical of polysaccharide that was chemically identified as GalNAc, whereas GalNAc was not detected in the control strain. Third, we have shown that SBA, which binds strongly to GalNAc and much weaker to galactose, reacted with purified crude Ssc from *E. coli* clones as well as from the cell wall of *S. aureus*. Finally,

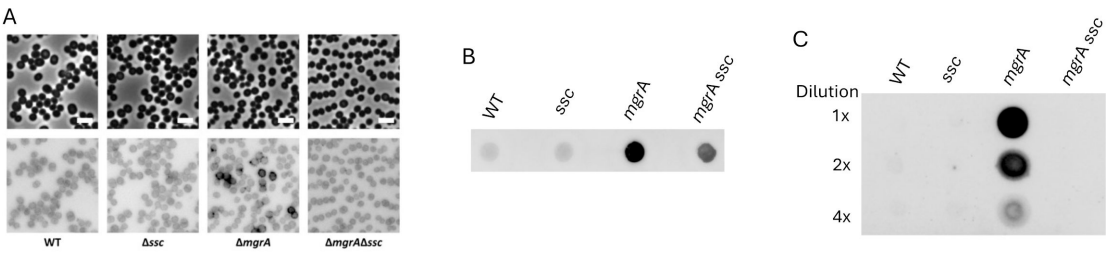

FIG 6 Detection of GalNAc. (A) *S. aureus* cells labeled with FITC-SBA: phase contrast images (top), and fluorescence micrographs (bottom). (B) Bacterial cells immobilized on nitrocellulose membrane and labeled with FITC-SBA. (C) Immunoblotting of purified *S aureus* cell wall fractions with biotin-SBA and HRP-streptavidin. WT, 8325-4; *ssc*, CYLA946; *mgrA*, CYL12670; *mgrA ssc*, CYLA958.

Downloaded from https://journals.asm.org/journal/jb on 25 June 2025 by 45.3.79.59.

we showed that Ssc was expressed on the *S. aureus* cell surface, as the expression of Ssc reduced phage adsorption as well as phage-induced cell lysis.

We initially attempted to identify the putative Ssc by comparing the carbohydrate compositions between the wild-type 8325-4 and the *ssc* mutant. However, we observed little or no significant difference in polysaccharide profiling in SDS-PAGE between the two strains (Fig. 1A), consistent with the weak *ssc* promoter under our growth conditions. Previously, we found that the multiple gene regulator MgrA was a strong repressor of *ssc*, and inactivation of MgrA increased the *ssc* expression by ~1,900 fold in strain Newman (5). The strong repression of *ssc* by MgrA was further confirmed by using the sfGFP reporter assay (Fig. 1B). This prompted us to compare the polysaccharide profiles between the *mgrA* mutant and the *mgrA-ssc* double mutant in an attempt to characterize the Ssc. However, we found a high level of polysaccharide-like materials in the *mgrA-ssc* double mutant. We, therefore, resorted to expressing the *ssc* genes in *E. coli* to characterize the Ssc polysaccharide. Our results suggest that Ssc is likely a poly-GalNAc. To our knowledge, this is the first report of a GalNAc-containing polysaccharide of *S. aureus*, although we are unable to determine the detailed structure at this stage.

In this study, we demonstrated that Ssc is surfaced-exposed by measuring phage accessibility to cell walls as well as by direct binding of FITC-SBA to cell surfaces or the purified cell wall fractions. Interestingly, we showed no difference in FITC-SBA binding between the wild-type and the *ssc* mutant, and positive binding was only detected in the *mgrA* mutant. On the other hand, the phage method was able to demonstrate the difference in Ssc surface exposure between the wild-type and the *ssc* mutant. These results suggest that Ssc is surface-exposed, and measuring phage accessibility to cell walls is a more sensitive method. In the phage assays, we also included the *mgrA* and *mgrA-ssc* mutant; however, the *ssc* mutation did not have an effect in the *mgrA* mutant background (not shown). As MgrA is a global regulator affecting a large number of genes, including those encoding cell surface proteins and proteases (5, 7), other factors regulated by MgrA likely play a more important role than Ssc in phage accessibility to the cell walls.

Surface polysaccharides play important roles in bacterial pathogenesis. To study the cellular functions of Ssc, we tested its role in biofilm formation. However, the results were inconclusive. In some experiments, we observed a weak effect on biofilm formation, but the results were insignificant in other experiments. The inconsistency is likely due to a very low expression level of the *ssc* genes or experimental conditions. Another possible role of Ssc is the involvement of host immune evasion, which requires further studies.

In *S. aureus*, the undecaprenyl-phosphate lipid carrier is required for the synthesis of peptidoglycan, capsular polysaccharides, and teichoic acids, but not for PIA (20–24). Although we lack experimental evidence confirming the involvement of this common cell membrane lipid carrier in Ssc synthesis, the results that Ssc could be produced in *E. coli* using the PGCT system support this metabolic pathway. In this process, a nucleotide-activated sugar component is first transferred to the lipid carrier catalyzed by a specific transferase that recognizes the nucleotide-activated sugar. The presence of the second gene in the *ssc* operon, *sscB*, which is highly homologous to various bacterial UDP *N*-acetylgalactosamine undecaprenyl-phosphate transferases, further supports the involvement of undecaprenyl-phosphate lipid carrier in the Ssc synthesis.

MATERIALS AND METHODS

Bacterial strains and culture condition

The bacterial strains and plasmids used in this study are listed in Table 2. *E. coli* XL1-blue and DH5α were used for plasmid construction and maintenance. Competent *S. aureus* RN4220 was used as the recipient for plasmid electroporation. Phage 80α or 52A was used for DNA transduction between *S. aureus* strains and also used for cell lysis and adsorption studies. *S. aureus* strains were cultured with tryptic soy broth (TSB), and *E. coli* strains were cultured in Luria-Bertani broth (LB) unless specified otherwise.

Downloaded from https://journals.asm.org/journal/jb on 25 June 2025 by 45.3.79.59.

Antibiotics were added to the culture medium, when necessary, at a final concentration of 100 µg/mL for ampicillin, 3 µg/mL for tetracycline, 30 µg/mL, or 50 µg/mL for kanamycin. Chloramphenicol was used at a final concentration of 10 µg/mL and 20 µg/mL for *S. aureus* and *E. coli* strains, respectively.

Strain and plasmid construction

Primers used for plasmid and strain construction are listed in Table S1. To construct a deletion mutant of *ssc* operon (CYLA946), DNA fragments flanking the operon were amplified by PCR from 8325-4 genomic DNA using primer pairs of ssc-KO1/ssc-KO2 and ssc-KO3/ssc-KO4. The *tetK* gene of pT181 was amplified with pTet1/pTet2 primers. The PCR fragments were cloned in tandem into plasmid pJB38 such that the deleted *ssc* operon was replaced with the *tetK* gene. To construct a markerless deletion mutant of *mgrA* (CYL13008), DNA fragments flanking the *mgrA* gene were amplified by PCR using primer pairs of mgrdc1/mgrdc4, mgrdc2/mgrdc3, followed by overlapping PCR using primer pair mgrdc1/mgrdc2. The fragment was cloned into pIMAY by SLIC method (33). To construct an *ssc* overexpression strain (CYL12674), DNA fragments were amplified from 8325-4 chromosomal DNA using primer pairs of attB2-sscP13/sscP8 and attB1-sscP12/sscP11. A P*cap1* promoter fragment was amplified from *S. aureus* M strain genomic DNA using sscP9/sscP10 primers. The amplified fragments were further assembled by overlapping PCR amplification and cloned into the pKOR-1 vector. All PCR inserts were verified by sequencing. Allelic replacement was performed as described previously (30). CYL12670 (8325-4 Δ*mgrA::cat*) was constructed by phage transduction from CYL1040 (25). All mutants were further verified by PCR.

To construct P*ssc-sfgfp* reporter plasmid pMLE283, the *ssc* promoter region (P*ssc*, 355 bp upstream and 85 bp downstream of SAOUHSC_00088 start codon) was PCR amplified using P88-2/P88-3 primers and cloned into the superfolder green fluorescent protein (sfGFP) reporter plasmid pMLE57 (32). To clone the entire *ssc* operon, the 8325-4 genomic DNA was first amplified by two primer pairs, PS-1F/PS-2R and PS-3F/PS-4R, representing 5′ half and 3′ half of the *ssc* gene cluster. The resultant fragments were separately cloned into pGEMT-easy and verified by sequencing. The two PCR fragments in pGEMT-easy were then digested with KpnI/NsiI and NsiI/SalI, respectively, and cloned into pBAD18 digested with KpnI and SalI. The intact *ssc* operon in pBAD18 was digested with KpnI and HindIII and then subcloned into similarly digested pBBR1MCS-2. The resultant plasmid pMLE254 was used for expressing Ssc and /or Ssc-AcrA-His_6 glycoconjugate in *E. coli*.

MAJ1625 (MG1655 λDE3 Δ*wecA* Δ*waaL*) is the glycoengineering strain for this study. Gene deletions were constructed in *E. coli* MG1655 by using lambda RED recombination (34) or P1-mediated transduction. Kanamycin resistance markers were excised by FLP recombinase produced from pCP20 (35). Gene deletions were verified by PCR. The O-antigen WaaL ligase was deleted to prevent Ssc from being transferred onto lipid-A-core. The initiating glycosyltransferase WecA was deleted to ensure synthesis of Ssc-AcrA by preventing PglB from transferring *E. coli* glycans initiating with GlcNAc (i.e., enterobacterial common antigen). The λDE3 prophage in MAJ1625 was introduced by using the λDE3 Lysogenization Kit (Novagen). The λDE3 prophage encodes an IPTG-inducible copy of T7 polymerase, which is required to express *pglB*-2xHA and ss-*dsbA*-^{4xDQNAT}*acrA*^{4xDQNAT}-*his_6* from pMAJ205.

pMAJ205 is a plasmid that expresses *pglB*-2xHA and ss-*dsbA*-^{4xDQNAT}*acrA*^{4xDQNAT}-*his_6* from $P_{T7\text{-}1}$ and $P_{T7\text{-}2}$ in pACYCDuet-1 (Novagen), respectively. Sequences corresponding to *C. jejuni pglB* and *acrA* were obtained from Biocyc (*C. jejuni* NCTC11168), codon optimized for expression in *E. coli* (using the IDT codon optimization tool) and synthesized by Epoch Life Sciences. We modified *pglB* at the C-terminus with two tandem repeats of the hemagglutinin sequence (2×HA) to enable detection. We modified *acrA* at the N-terminus with the signal peptide from DsbA (for localization to the periplasm) and four tandem repeats of DQNAT (glycosylation motif). We also modified *acrA* at the C-terminus with four tandem repeats of DQNAT and a 6×His-tag for purification. The

Downloaded from https://journals.asm.org/journal/jb on 25 June 2025 by 45.3.79.59.

TABLE 2 Strains and plasmids

Strain or plasmid	Relevant characteristics	Reference or source
S. aureus strains		
RN4220	Restriction negative laboratory strain	Iandolo
8325-4	Prophage-free laboratory strain	Iandolo
CYL1040	Becker Δ*mgrA*::*cat*	25
CYLA946	8325-4 Δ*ssc*::*tetK*	This study
CYL12670	8325-4 Δ*mgrA*::*cat*	This study
CYL12674	8325-4 P*cap1*:*ssc*	This study
CYL13008	8325-4 Δ*mgrA*	This study
CYLA958	8325-4 Δ*mgrA*::*cat* Δ*ssc*::*tetK*	This study
E. coli strains		
XL1-Blue	Host strain for plasmids	Strategene
DH5α	Host strain for plasmids	Invitrogen
MG1655	F^- λ^- *ilvG rfb*-50 *rph*-1	26
CYLE259	MG1655 (pBBR1MCS-2)	This study
CYLE260	MG1655 (pMLE254)	This study
MAJ1625	MG1655 λDE3 Δ*wecA*::*frt* Δ*waaL*::*frt*	This study
MAJ1626	MAJ1625 (pMAJ205)	This study
CYLE276	MAJ1626 (pBBR1MCS-2)	This study
CYLE277	MAJ1626 (pMLE254)	This study
Plasmids		
pGEM-T easy	*E. coli* cloning vector	Promega
pBAD18	*E. coli* expressing vector	27
pBBR1MCS-2	*E. coli* expression vector	28
pMAJ205	pACYCDuet-1::*pglB*-2xHA ss-*dsbA*-^{4xDQNAT}-*acrA*^{4xDQNAT}-*his*$_6$	This study
pMLE254	pBBR1MCS-2-*ssc*	This study
pJB38	Vector for allele replacement	29
pKOR1	Vector for allele replacement	30
pIMAY	Vector for allele replacement	31
pMLE57	pLI50 with *sfgfp*	32
pMLE283	pMLE57-P*ssc*	This study

synthesized ss-*dsbA*-^{4xDQNAT}acrA^{4xDQNAT}-*his*$_6$ construct was amplified using primers P1264 and P1292. The 1,399 bp product was cut with NdeI and PacI and ligated to the same sites of pACYCDuet-1. The synthesized *pglB*-2xHA construct was amplified using primers P1308 and P1309. The 2,225 bp product was cut with NcoI and SacI and ligated to the same sites of the pACYCDuet-1::ss-*dsbA*-^{4xDQNAT}*acrA*^{4xDQNAT}-*his*$_6$ intermediate plasmid.

Heat-extraction of SsC carbohydrate from *S. aureus*

Overnight cultures of *S. aureus* strains were centrifuged, washed with 1 mL phosphate-buffered saline (PBS), and resuspended in 200 µL PBS (OD_{600}, ~10). The suspension was subjected to heat extraction in a boiling water bath for 2 h and centrifugation. Supernatants were treated with RNase A, DNase I, and then proteinase K.

Western blot

Carbohydrate fractions were dot-blotted to nitrocellulose paper or resolved in SDS-PAGE and transferred to PVDF membrane. The blots were incubated with biotinylated SBA (Vector Laboratories) and streptavidin-horseradish peroxidase (HRP) (Thermo Scientific) and detected with ChemiDoc XRS + System (Bio-Rad Laboratories, Hercules, CA) using chemiluminescent HRP substrate (Thermo Scientific). For detecting AcrA-His_6, the blots were incubated with anti-His mouse mAB 27E8 (Cell Signaling), followed by HRP-conjugated goat anti-mouse IgG (Invitrogen). The blots were developed as above.

Downloaded from https://journals.asm.org/journal/jb on 25 June 2025 by 45.3.79.59.

Heat extraction of polysaccharide from *E. coli*

Overnight cultures of CYLE259 and CYLE260 (LB 50 µg/mL Kanamycin) were diluted with Super Optimal broth (SOB) medium containing 30 µg/mL Kanamycin and 1 mM IPTG to OD_{600} of 0.08 and incubated at 28°C with shaking at 225 rpm for 24 h. Bacterial cells were collected by centrifugation. Cells were then suspended to OD_{600} of 75 per mL with 1× Tris EDTA (TE) (pH 8.0), and heat treated in a boiling water bath for 2 h. Supernatants were collected after centrifugation, treated with TCA (20% wt/vol) on ice for 30 min to precipitate proteins and nucleic acids, and further centrifuged at 18,000 × *g* at 4°C for 30 min. Polysaccharide fractions in the supernatants were precipitated with ethanol (2.5 vol/vol) at −20°C for 24 h. After centrifugation at 18,000 × *g* at 4°C for 30 min, the pellet was washed with cold ethanol two times, air dried, and dissolved with sterile milliQ water.

Glycan expression from *E. coli*

E. coli strains (CYLE276 and/or CYLE277) were cultured at 28°C for 24 h in SOB medium containing chloramphenicol (20 µg/mL) and kanamycin (50 µg/mL) and 1 mM IPTG. Cell pellets were lysed in Solulyse solution (Genlantis) and lysozyme (0.4 µg/µL). Ssc-AcrA-His_6 glycoconjugates were further purified by using His-Bind resin (Novagen).

Carbohydrate mass spectral analysis

Glycosyl composition analysis

Glycosyl composition analysis was performed by combined gas chromatography-mass spectrometry (GC-MS) of the per-O-trimethylsilyl (TMS) derivatives of the monosaccharide methyl glycosides produced from the sample by acidic methanolysis as described previously by Coleman et al. (36). Briefly, the samples were hydrolyzed in 400 µL 1M methanolic HCl overnight at 80°C. The dried samples were then re-N-acetylated using a mixture of methanol:acetic anhydride:pyradine (2:1:1) at room temperature for 20 min. The samples were further derivatized with Tri-Sil (ThermoFisher Scientific) at 80°C for 30 min. GC-MS analysis of the TMS methyl glycosides was performed on an Agilent 7890A GC interfaced to a 5975C MSD, using a Supelco Equity-1 fused silica capillary column (30 m × 0.25 mm ID).

Glycoproteomics

Gel fragments were cut into pieces of ~1 mm each with a sterile scalpel. After cutting, gel pieces were transferred info Eppendorf tubes, and 500 µL acetonitrile (ACN): NH4HCO3 (AmBic) (1:1) was added. After addition of ACN:AmBic buffer, gel pieces were incubated at room temperature for 30 min. This step was repeated four times in order to remove all Coomassie dye from the gel pieces. The destained gel pieces were shrunk by adding 500 µL ACN and incubating at room temperature for 30 min. The ACN was removed, and 300 µL of 25 mM dithiothreitol (DTT) in water was added to the tubes to reduce the protein by incubation at 56°C for 30 min. The DTT solution was removed by adding 500 µL ACN and pipetting out the liquid. Three hundred milliliters of 90 mM iodoacetamide (IAA) was added to the gel and allowed to incubate in the dark for 20 min (alkylation). The IAA solution was removed in a similar manner by the addition of acetonitrile and the removal of the liquid. To digest the reduced and alkylated protein, a final addition of 5 µg sequencing grade trypsin in AmBic (~1:5 ratio/ protein:enzyme) was added to the gel. Tryptic digestion was performed for 18 h at 37°C. To release the tryptic peptides, 500 µL of 1:2/H_2O:ACN plus 5% formic acid was added to the gels and allowed to incubate at room temperature for 15 min. This procedure was repeated two times, and all supernatant was collected into new tubes. Collected supernatant (~1.5 mL) was dried in a SpeedVac. Any active trypsin that remained was deactivated by heating to 100°C for 5 min. Trytpic glycopeptides were finally resuspended with 50 µL AmBic buffer each and filtered on 0.2 µm filter prior to liquid chromatography tandem mass spectrometry (LC-MS/MS) analysis (37).

Downloaded from https://journals.asm.org/journal/jb on 25 June 2025 by 45.3.79.59.

LC-MS/MS analysis

The glycopeptides were analyzed on an Ultimate 3000 RSLCnano (ThermoFisher Scientific) connected to a Thermo Eclipse Fusion Orbitrap mass spectrometer (ThermoFisher Scientific). Commercial C18 nano-LC columns (150 mm × 75 µm; 3 µm packing) were used for chromatographic separation. The separation conditions were linearly lowered to 80% acetonitrile in a solution containing 0.1% formic acid over 180 min. A data-dependent program was used for acquisition where the precursor ion scan was acquired at 120 k resolution followed by top-down fragmentation of high-to-low intensity m/z by stepped higher collisional dissociation (HCD) [collision energy (%) = 20,30,40] at 30 k resolution within 3 s. Charge state screening was enabled, and precursors with an unknown charge state or a charge state of +1 were excluded from fragmentation. Dynamic exclusion was enabled (exclusion duration of 30 s) (38).

Byonic searches and filtering of the data

The resulting glycoproteomic data were processed with Byonic (v4.0.12) and searched against the provided amino acid sequence and a custom library of N-glycans. The precursor mass tolerance and fragment mass tolerances were set to 5 ppm and 10 ppm, respectively. Additional dynamic modifications including deamidation of N and Q, carboxymethylation of C, and oxidation of glycopeptide precursor were also included in the search. Assignments were made using Byonic software and manual interpretation using FreeStyle 1.8 (ThermoFisher Scientific).

Isolation of *S. aureus* cell wall fraction

S. aureus cell wall fractions were prepared as described by Pieper et al. (39) in the presence of 27% sucrose and lysostaphin. Isolated cell wall samples were further treated with proteinase K.

Phage adsorption

Overnight cultures in TSB were diluted with fresh medium to OD_{600} of 0.05 and incubated at 37°C, 225 rpm for 80 min. Cultures (about 3×10^7 CFU in 200 µL) were incubated with phage 52 A or 80α (about 3×10^6 PFU) at 37°C for 15 and 30 min. Unbound free phages ($P_{unbound}$) were separated from bound phages by centrifugation. Adsorption was calculated by taking the PFU of the unbound phage and subtracting it from PFU of the Input (P_{input}). Percent adsorption = $(P_{input} - P_{unbound})/P_{input}$.

Phage-induced cell lysis of *S. aureus*

Overnight *S. aureus* cultures in TSB were diluted with fresh TSB media to OD_{600} of 0.05 and incubated at 37°C in a rotary shaker at 225 rpm to OD_{600} of about 0.2. Cultures were incubated with phage 52 A, or 80α (MOI of 1:1) at 37°C with 175 rpm rotation. OD_{600} of each culture was monitored every 30 min for 5 h.

Labeling of fluorescein isothiocyanate-SBA

Whole-cell labeling with FITC-SBA for microscopy was carried out essentially as described by Jorgenson and Young (40). Briefly, overnight cultures were washed twice in PBS, incubated with 20 µg/mL FITC-SBA (Vector Laboratories) for 30 min, and washed twice again in PBS. The labeled cells were visualized by phase contrast and fluorescence microscopy.

SBA-FITC dot blot was carried out as described by Kay et al. (41) with minor modifications. An equivalent amount of *S. aureus* cell (1 mL of OD_{600} = 1.0) from overnight cultures was collected by centrifugation and suspended with 20 µL PBS. Aliquots of 3 µL were spotted on the nitrocellulose membrane and dried overnight at room temperature. Membranes were blocked with 5% bovine serum albumin (BSA) in PBS and labeled with 20 µg/mL of SBA-FITC in blocking reagent.

Downloaded from https://journals.asm.org/journal/jb on 25 June 2025 by 45.3.79.59.

ACKNOWLEDGMENTS

The authors thank Joseph Bryant for technical assistance and Anik Barman for critically reading the manuscript.

This work is supported by grants from the National Institutes of Health (AI159212 to CYL and P20GM103625 to M.A.J.). E.J.R. was supported by NIGMS training grant award R25GM083247. The authors also acknowledge the UAMS sequencing core supported in part by National Institutes of Health grant P20GM103625. The mass spectrometry part of this research was supported in part by the National Institutes of Health (NIH) (R24GM137782) to P.A. as well as supported by GlycoMIP, a National Science Foundation Materials Innovation Platform funded through Cooperative Agreement DMR-1933525.

AUTHOR AFFILIATIONS

[1]Department of Microbiology and Immunology, University of Arkansas for Medical Sciences, Little Rock, Arkansas, USA
[2]Complex Carbohydrate Research Center, University of Georgia, Athens, Georgia, USA

AUTHOR ORCIDs

Chia Y. Lee http://orcid.org/0000-0002-2503-5467

FUNDING

Funder	Grant(s)	Author(s)
HHS | NIH | National Institute of Allergy and Infectious Diseases (NIAID)	AI159212	Mei G. Lei Chia Y. Lee
HHS | NIH | National Institute of General Medical Sciences (NIGMS)	P20GM103625	Matthew A. Jorgenson
HHS | NIH | National Institute of General Medical Sciences (NIGMS)	P20GM083247	Emily J. Robbs
HHS | NIH | National Institute of General Medical Sciences (NIGMS)	R24GM137782	Ian M. Black Stephanie Archer-hartmann Sergei shalygin Parastoo Azadi
National Science Foundation (NSF)	DRM-1933525	Parastoo Azadi

ADDITIONAL FILES

The following material is available online.

Supplemental Material

Supplemental material (JB00048-24-S0001.docx). Table S1; Figures S1 to S5.

REFERENCES

1. Tong SYC, Davis JS, Eichenberger E, Holland TL, Fowler VG. 2015. *Staphylococcus aureus* infections: epidemiology, pathophysiology, clinical manifestations, and management. Clin Microbiol Rev 28:603–661. https://doi.org/10.1128/CMR.00134-14
2. O'Riordan K, Lee JC. 2004. *Staphylococcus aureus* capsular polysaccharides. Clin Microbiol Rev 17:218–234. https://doi.org/10.1128/CMR.17.1.218-234.2004
3. Cerca N, Jefferson KK, Maira-Litrán T, Pier DB, Kelly-Quintos C, Goldmann DA, Azeredo J, Pier GB. 2007. Molecular basis for preferential protective efficacy of antibodies directed to the poorly acetylated form of staphylococcal poly-*N*-acetyl-β-(1-6)-glucosamine. Infect Immun 75:3406–3413. https://doi.org/10.1128/IAI.00078-07
4. Gillaspy AF, Worrell V, Orvis J, Roe BA, Dyer DW, Iandolo JJ. 2006. The *Staphylococcus aureus* NCTC 8325 genome. In Fischetti VA, Novick RP, Ferretti JJ, Portnoy DA, Rood JI (ed), Gram-positive pathogens, 2nd ed. Vol. 381–412. American Society for Microbiology, Washington, DC.
5. Luong TT, Dunman PM, Murphy E, Projan SJ, Lee CY. 2006. Transcription profiling of the *mgrA* regulon in *Staphylococcus aureus*. J Bacteriol 188:1899–1910. https://doi.org/10.1128/JB.188.5.1899-1910.2006
6. Manna AC, Ingavale SS, Maloney M, van Wamel W, Cheung AL. 2004. Identification of *sarV* (SA2062), a new transcriptional regulator, is repressed by SarA and MgrA (SA0641) and involved in the regulation of autolysis in *Staphylococcus aureus*. J Bacteriol 186:5267–5280. https://doi.org/10.1128/JB.186.16.5267-5280.2004

Downloaded from https://journals.asm.org/journal/jb on 25 June 2025 by 45.3.79.59.

7. Crosby HA, Schlievert PM, Merriman JA, King JM, Salgado-Pabón W, Horswill AR. 2016. The *Staphylococcus aureus* global regulator MgrA modulates clumping and virulence by controlling surface protein expression. PLoS Pathog 12:e1005604. https://doi.org/10.1371/journal.ppat.1005604
8. Wann ER, Dassy B, Fournier JM, Foster TJ. 1999. Genetic analysis of the *cap5* locus of *Staphylococcus aureus*. FEMS Microbiol Lett 170:97–103. https://doi.org/10.1111/j.1574-6968.1999.tb13360.x
9. Cue D, Lei MG, Luong TT, Kuechenmeister L, Dunman PM, O'Donnell S, Rowe S, O'Gara JP, Lee CY. 2009. Rbf promotes biofilm formation by *Staphylococcus aureus* via repression of *icaR*, a negative regulator of *icaADBC*. J Bacteriol 191:6363–6373. https://doi.org/10.1128/JB.00913-09
10. Pozzi C, Waters EM, Rudkin JK, Schaeffer CR, Lohan AJ, Tong P, Loftus BJ, Pier GB, Fey PD, Massey RC, O'Gara JP. 2012. Methicillin resistance alters the biofilm phenotype and attenuates virulence in *Staphylococcus aureus* device-associated infections. PLoS Pathog 8:e1002626. https://doi.org/10.1371/journal.ppat.1002626
11. Jenni R, Berger-Bächi B. 1998. Teichoic acid content in different lineages of *Staphylococcus aureus* NCTC8325. Arch Microbiol 170:171–178. https://doi.org/10.1007/s002030050630
12. Sharma V, Srinivas VR, Adhikari P, Vijayan M, Surolia A. 1998. Molecular basis of recognition by Gal/GalNac specific legume lectins: influence of Glu 129 on the specificity of peanut agglutinin (PNA) towards C2-substituents of galactose. Glycobiology 8:1007–1012. https://doi.org/10.1093/glycob/8.10.1007
13. Kay E, Cuccui J, Wren BW. 2019. Recent advances in the production of recombinant glycoconjugate vaccines. NPJ Vaccines 4:16. https://doi.org/10.1038/s41541-019-0110-z
14. Chen MM, Glover KJ, Imperiali B. 2007. From peptide to protein: comparative analysis of the substrate specificity of N-linked glycosylation in *C. Jejuni*. Biochemistry 46:5579–5585. https://doi.org/10.1021/bi602633n
15. Wilkinson BJ, Holmes KM. 1979. *Staphylococcus aureus* cell surface: capsule as a barrier to bacteriophage adsorption. Infect Immun 23:549–552. https://doi.org/10.1128/iai.23.2.549-552.1979
16. Luong TT, Lee CY. 2002. Overproduction of type 8 capsular polysaccharide augments *Staphylococcus aureus* virulence. Infect Immun 70:3389–3395. https://doi.org/10.1128/IAI.70.7.3389-3395.2002
17. Xia G, Corrigan RM, Winstel V, Goerke C, Gründling A, Peschel A. 2011. Wall teichoic acid-dependent adsorption of staphylococcal siphovirus and myovirus. J Bacteriol 193:4006–4009. https://doi.org/10.1128/JB.01412-10
18. Jurado A, Fernández L, Rodríguez A, García P. 2022. Understanding the mechanisms that drive phage resistance in staphylococci to prevent phage therapy failure. Viruses 14:1061. https://doi.org/10.3390/v14051061
19. Keinhörster D, George SE, Weidenmaier C, Wolz C. 2019. Function and regulation of *Staphylococcus aureus* wall teichoic acids and capsular polysaccharides. Int J Med Microbiol 309:151333. https://doi.org/10.1016/j.ijmm.2019.151333
20. Higashi Y, Strominger JL, Sweeley CC. 1970. Biosynthesis of the peptidoglycan of bacterial cell walls: XXI. isolation of free C55-isoprenoid alcohol and of lipid intermediates in peptidoglycan synthesis from *Staphylococcus aureus*. J Biol Chem 245:3697–3702.
21. Sandermann H, Strominger JL. 1972. Purification and properties of C55-Isoprenoid alcohol phosphokinase from *Staphylococcus aureus*. J Biol Chem 247:5123–5131. https://doi.org/10.1016/S0021-9258(19)44948-X
22. Watkinson RJ, Hussey H, Baddiley J. 1971. Shared lipid phosphate carrier in the biosynthesis of teichoic acid and peptidoglycan. Nat New Biol 229:57–59. https://doi.org/10.1038/newbio229057a0
23. Rausch M, Deisinger JP, Ulm H, Müller A, Li W, Hardt P, Wang X, Li X, Sylvester M, Engeser M, Vollmer W, Müller CE, Sahl HG, Lee JC, Schneider T. 2019. Coordination of capsule assembly and cell wall biosynthesis in *Staphylococcus aureus*. Nat Commun 10:1404. https://doi.org/10.1038/s41467-019-09356-x
24. Gerke C, Kraft A, Süssmuth R, Schweitzer O, Götz F. 1998. Characterization of the N-acetylglucosaminyltransferase activity involved in the biosynthesis of the *Staphylococcus epidermidis* polysaccharide intercellular adhesin. J Biol Chem 273:18586–18593. https://doi.org/10.1074/jbc.273.29.18586
25. Luong TT, Newell SW, Lee CY. 2003. Mgr, a novel global regulator in *Staphylococcus aureus*. J Bacteriol 185:3703–3710. https://doi.org/10.1128/JB.185.13.3703-3710.2003
26. Jensen KF. 1993. The *Escherichia coli* K-12" wild types" W3110 and MG1655 have an *rph* frameshift mutation that leads to pyrimidine starvation due to low *pyrE* expression levels. J Bacteriol 175:3401–3407. https://doi.org/10.1128/jb.175.11.3401-3407.1993
27. Guzman LM, Belin D, Carson MJ, Beckwith JO. 1995. Tight regulation, modulation, and high-level expression by vectors containing the arabinose PBAD promoter. J Bacteriol 177:4121–4130. https://doi.org/10.1128/jb.177.14.4121-4130.1995
28. Kovach ME, Elzer PH, Hill DS, Robertson GT, Farris MA, Roop RM, Peterson KM. 1995. Four new derivatives of the broad-host-range cloning vector pBBR1MCS, carrying different antibiotic-resistance cassettes. Gene 166:175–176. https://doi.org/10.1016/0378--1119(95)00584-1
29. Bose JL, Fey PD, Bayles KW. 2013. Genetic tools to enhance the study of gene function and regulation in *Staphylococcus aureus*. Appl Environ Microbiol 79:2218–2224. https://doi.org/10.1128/AEM.00136-13
30. Bae T, Schneewind O. 2006. Allelic replacement in *Staphylococcus aureus* with inducible counter-selection. Plasmid 55:58–63. https://doi.org/10.1016/j.plasmid.2005.05.005
31. Monk IR, Shah IM, Xu M, Tan MW, Foster TJ. 2012. Transforming the untransformable: application of direct transformation to manipulate genetically *Staphylococcus aureus* and *Staphylococcus epidermidis*. mBio 3:e00277-11. https://doi.org/10.1128/mBio.00277-11
32. Lei MG, Lee CY. 2020. Mgra activates staphylococcal capsule via SigA-dependent promoter. J Bacteriol 203:e00495-20. https://doi.org/10.1128/JB.00495-20
33. Li MZ, Elledge SJ. 2007. Harnessing homologous recombination *in vitro* to generate recombinant DNA via SLIC. Nat Methods 4:251–256. https://doi.org/10.1038/nmeth1010
34. Datsenko KA, Wanner BL. 2000. One-step inactivation of chromosomal genes in *Escherichia coli* K-12 using PCR products. Proc Natl Acad Sci USA 97:6640–6645. https://doi.org/10.1073/pnas.120163297
35. Cherepanov PP, Wackernagel W. 1995. Gene disruption in *Escherichia coli*: TC^R and km^R cassettes with the option of Flp-catalyzed excision of the antibiotic-resistance determinant. Gene 158:9–14. https://doi.org/10.1016/0378-1119(95)00193-a
36. Coleman CM, Auker KM, Killday KB, Azadi P, Black I, Ferreira D. 2019. Arabinoxyloglucan oligosaccharides may contribute to the antiadhesive properties of porcine urine after cranberry consumption. J Nat Prod 82:589–605. https://doi.org/10.1021/acs.jnatprod.8b01043
37. Shajahan A, Heiss C, Ishihara M, Azadi P. 2017. Glycomic and glycoproteomic analysis of glycoproteins—a tutorial. Anal Bioanal Chem 409:4483–4505. https://doi.org/10.1007/s00216-017-0406-7
38. Shajahan A, Pepi LE, Rouhani DS, Heiss C, Azadi P. 2021. Glycosylation of SARS-CoV-2: structural and functional insights. Anal Bioanal Chem 413:7179–7193. https://doi.org/10.1007/s00216-021-03499-x
39. Pieper R, Gatlin-Bunai CL, Mongodin EF, Parmar PP, Huang S-T, Clark DJ, Fleischmann RD, Gill SR, Peterson SN. 2006. Comparative proteomic analysis of *Staphylococcus aureus* strains with differences in resistance to the cell wall - targeting antibiotic vancomycin. Proteomics 6:4246–4258. https://doi.org/10.1002/pmic.200500764
40. Jorgenson MA, Young KD. 2016. Interrupting biosynthesis of O antigen or the lipopolysaccharide core produces morphological defects in *Escherichia coli* by sequestering undecaprenyl phosphate. J Bacteriol 198:3070–3079. https://doi.org/10.1128/JB.00550-16
41. Kay EJ, Dooda MK, Bryant JC, Reid AJ, Wren BW, Troutman JM, Jorgenson MA. 2024. Engineering *Escherichia coli* for increased Und-P availability leads to material improvements in glycan expression technology. Microb Cell Fact 23:72. https://doi.org/10.1186/s12934-024-02339-8

Downloaded from https://journals.asm.org/journal/jb on 25 June 2025 by 45.3.79.59.